

Immunohistochemical expression status of p53, CD44v9 and Ki-67 in a series of fallopian tube lesions of high-grade serous carcinoma.

Sumire Sugimoto 1), Tomoko Uchiyama 1), Naoki Kawahara 2), Chiho Ohbayashi 2), Hiroshi Kobayashi 1).

1. Department of Diagnostic Pathology, Nara Medical University, Kashihara, Japan.
2. Department of Obstetrics and Gynecology, Nara Medical University, Kashihara, Japan.

Running Title:

Changes in CD44v9 expression in fallopian tube precursor lesions of HGSC.

Word count: 3094 words (excluding abstract and references)

Corresponding author:

Sumire Sugimoto, MD.

Department of Diagnostic Pathology, Nara Medical University,

840 Shijo-cho, Kashihara, 634-8522, Nara, Japan.

Tel, +81-744-29-8910; Fax, +81-744-29-1460; Email, sumire6003@naramed-u.ac.jp

ORCID:0000-0001-5049-3227

Conflicts of interest and Source of Funding :

The authors declared no potential conflicts of interest with respect to the research, authorship and publication of this article.

This work was supported by JSPS KAKENHI Grant Number JP16K11150, 18K09269 and 18K09234.

Abstract

Background:

Pelvic high-grade serous carcinoma (HGSC) has been postulated to arise via a stepwise accumulation of (epi)genetic alterations through secretory cell outgrowth (SCOUT), p53 signature, and serous tubal intraepithelial carcinoma (STIC) to invasive HGSC. The aim of this study is to investigate the alterations in the p53 and CD44v9 expression and the status of Ki-67 labeling index in a series of fallopian tube lesions of HGSC patients.

Methods:

A total of 45 specimens were analyzed in 16 patients with HGSC, and their lesions were categorized as follows: morphologically normal fallopian tube epithelium (FTE, n=6 samples), SCOUT (n = 5), p53 signature (n = 4), dormant STIC (n = 8), active STIC (n = 6), and HGSC (n = 16). Morphological features and immunohistochemical expression patterns of p53 protein, CD44v9 protein and Ki-67 antigen were blindly evaluated by two pathologists.

Results:

Increased nuclear p53 protein accumulation was observed in the p53 signature, dormant STIC, active STIC and HGSC compared with normal FTE and SCOUT ($P < 0.001$). Immunohistochemistry (IHC) scores of CD44v9 protein expression were significantly higher in normal FTE, SCOUT and p53 signature than in dormant STIC, active STIC and HGSC ($P < 0.001$). Both active STIC and HGSC had significantly higher Ki-67 labeling indices than normal FTE, SCOUT, p53 signature and dormant STIC ($P < 0.001$). CD44v9 loss contributes to the stepwise progression of p53 signature to dormant STIC.

Conclusions:

In conclusion, the p53 mutation followed by CD44v9 loss may be involved in the evolution of STIC, which may confer positive clonal selection with a growth and survival advantage.

Key words: TP53; CD44v9; Ki-67; Serous tubal intraepithelial carcinoma (STIC); High grade serous carcinoma (HGSC).

Introduction

It is widely accepted that pelvic high-grade serous carcinoma (HGSC) develops through multistep (epi)genetic mutations from precursor lesions in the distal portion of the fallopian tube ¹⁻⁸. Putative precursor lesions of HGSC include secretory cell outgrowth (SCOUT), p53 signatures and serous tubal intraepithelial carcinoma (STIC), which would progress to invasive HGSC ^{1,9}. The SCOUT is defined as a discrete expansion of at least 30 secretory cells without p53 nuclear staining ¹⁰. p53 signature is defined as benign-appearing tubal epithelial cells with p53 protein accumulation and proposed as a tubal precursor for STIC ¹¹. STIC is an intraepithelial noninvasive lesion showing significant atypia that is formed in the distal fallopian tube epithelium (FTE) and plays a key role in the early stages of HGSC carcinogenesis ¹². Based on the proliferative activity, STIC lesions are divided into two types: dormant STIC (or serous tubal intraepithelial lesion [STIL]) and active STIC (or proliferative STIC) that can be characterized by differential staining of Ki-67 antigen ¹³. Although recent genomic and molecular data are transforming our understanding of the steps of HGSC tumorigenesis and their relationship to one another ^{2-7,13}, the detailed sequence of (epi)genetic alterations in the carcinogenesis process remains unknown.

Epidemiological studies showed that incessant ovulation and repeated hemorrhage have been linked to the development of HGSC ^{9,14}. Ovulation fluid and hemorrhage contain prostaglandins, hemoglobin, heme, and iron, which induce reactive oxygen species (ROS). Excessive oxidative stress can cause increased DNA damage and impaired DNA repair ⁹. To establish a redox balance, cells exert antioxidant defense systems that detoxify elevated ROS levels ¹⁵. Dysregulation of ROS due to reduced antioxidant defense systems may be an important etiological factor for the accumulation of (epi)genetic alterations in precancerous lesions, leading to HGSC tumorigenesis ⁹. Among a variety of proteins involved in the redox regulation, we focused on the expression of CD44v9, a splice variant isoform of CD44. CD44v9 stabilizes the glutamate-cystine transporter xCT (also known as SLC7A11 [solute carrier family 7 member 11]), thereby inducing de novo synthesis of glutathione antioxidant peptide inside cells and decreasing intracellular levels of ROS ¹⁶. Down-regulation of CD44v9 protein may be associated with malignant transformation of endometriosis, including ovarian clear cell carcinoma and endometrioid carcinoma ¹⁷. However, there have been no reports on the spatial and temporal expression of CD44v9 during the multi-stage carcinogenesis or stepwise progression from precursor lesions to HGSC. The aim of this study is to evaluate the morphological features and immunohistochemical expression status of p53, CD44v9 and Ki-67 in HGSC tumorigenesis. We found for the first time that CD44v9 loss may be an early event during the stepwise progression from p53 signature to dormant STIC.

Materials and Methods

Patient and tissue samples

Approval was obtained from the Nara Medical University Institutional Ethics Review Board (no. 2575). The study complied with the Declaration of Helsinki. Written informed consent was obtained from all

patients.

Following institutional review board approval, patients with primary pelvic HGSC who attended Nara Medical University Hospital, Kashihara, Japan from January 2015 to December 2017 were surveyed. Exclusion criteria were patients who received preoperative chemotherapy or immunotherapy. A total of 45 formalin-fixed paraffin-embedded specimens from 16 patients with HGSC (10 ovarian, 4 peritoneal and 2 fallopian tube carcinoma) were obtained from the surgical pathology archives. Their fallopian tube lesions were categorized as follows: morphologically normal FTE (n=6 samples), SCOUT (n = 5), p53 signature (n = 4), dormant STIC (n = 8), active STIC (n = 6), and HGSC (n = 16). For example, if a lesion with 'p53 signature' and a lesion with 'active STIC' were present on one slide, we counted the number of lesions as two. There were only 6 lesions in which morphologically normal FTE was observed in HGSC patients. Therefore, morphologically normal FTE from 5 patients who underwent total hysterectomy and salpingo-oophorectomy for benign diseases (uterine fibroids) were included in the analysis as a control. A total of 11 normal FTE specimens were examined. These patients were diagnosed with sporadic ovarian cancer because none of them met the criteria for hereditary breast and ovarian cancer (HBOC). All precursor lesions adjacent to normal-appearing FTE were discontinuous with HGSC in any slide analyzed. The definitions of SCOUT, p53 signature and STIC have been reported in refs. ^{10,11,13,18}. Dormant STIC is morphologically similar to serous tubal intraepithelial lesion (STIL), characterized by cytological atypia and low proliferative activity (Ki-67 labeling index <10%) ¹³. Active STIC is a pathomorphologically (significant nuclear atypia and architectural alterations) and immunohistochemically (p53 protein accumulation and high Ki-67 labeling index $\geq 10\%$) detectable lesion, located in the fimbriated end of the fallopian tube in most patients ¹³.

Immunohistochemical staining

These specimens were fixed in 10% buffered formalin and embedded in paraffin. The standard tissue paraffin block was sectioned at 4 μm for immunohistochemistry. Prior to staining, sections were deparaffinized in xylene and rehydrated in ethanol. After pretreatment using a microwave with 10 mM citrate buffer, pH 6.0, at 95°C for 20 minutes, sections were incubated with 3% hydrogen peroxide for 5 min to quench endogenous peroxidase and then incubated with the primary antibody overnight at 4°C. The primary antibodies used included mouse monoclonal anti-p53 (dilution, 1:50; clone DO-7, NCL-p53-DO7, Leica Biosystems, Newcastle, United Kingdom), mouse monoclonal anti-human Ki-67 antigen (dilution, 1:2; clone MIB-1, IS626, Dako, CA, USA) and mouse monoclonal anti-CD44v9 antibody (dilution, 1:400; clone CD44v9, Cat No. GTX34523, GeneTex, CA, USA). As a control for nonspecific binding of the secondary detection system, a slide in which control mouse or rabbit immunoglobulin G (Dako) was applied instead of the primary antibody was included from each block. Specimens of squamous cell carcinoma of the uterine cervix served as an equivalent positive control. Positive and negative controls were routinely included. The Envision⁺ solution for mouse and rabbit (Dako) was then applied for 30 minutes at room

temperature. The reaction products were observed using 3-3'-diaminobenzidine tetrahydrochloride (Sigma Chemical Company, St. Louis, Mo) and H₂O₂. The sections were then lightly counterstained with hematoxylin.

Assessment of immunohistochemical staining.

Protein expression was independently evaluated by two pathologists (Sumire Sugimoto and Tomoko Uchida) who were blinded to all of the clinicopathological variables. p53 immunostaining shows at least three staining patterns (overexpression, complete absence, normal/wild-type). The results of p53 immunostaining were interpreted according to ref. ¹⁹. Overexpression, complete absence or normal/wild type staining predicted gain-of-function, loss-of-function (stopgain, indel, splicing) or no detectable TP53 mutations, respectively ²⁰. Cells showing nuclear staining of p53 were considered to be positive, whereas cells without nuclear staining or with cytoplasmic staining were considered to be negative. The percentage of cells with positive immunostaining was tabulated in each lesion. The p53 positivity was defined as a distinct nuclear immunoreaction in >75% of the cells of the sample. In three samples, p53 expression was completely absent, which was interpreted as abnormal/mutation-type and recorded as 'positive' (**Supplemental Table1**). The CD44v9 positivity was evaluated as a semiquantitative immunohistochemical (IHC) staining score as described previously ²¹. Immunostaining intensity was classified as 0 (absent), 1 (weak, positivity observed at 400x), 2 (intermediate, positivity observed at 100x), or 3 (strong, positivity observed at 40x). The percentage of cells (from 0 to 100) was multiplied by the corresponding intensity (from 0 to 3) to obtain IHC score in the range of 0 to 300 ²¹. The Ki-67 positivity (Ki-67 labeling index) was defined as a distinct nuclear immunoreaction in $\geq 10\%$ of the cells within each lesion ²².

Statistical Analysis

Statistical analysis was conducted using SPSS software (version 22.0, SPSS Inc., Chicago, IL). Not all of IHC scores in groups, categorized fallopian tube lesions and HGSC, show normal distribution by using Shapiro-Wilk analysis. The significance of the difference of the immunohistochemical expression status Differences of IHC score among groups were analyzed by Kruskal-Wallis test. For significant Kruskal-Wallis tests, pairwise comparisons utilized the Steel-Dwass test. Further, Mann-Whitney U test was used comparing between two groups. The optimal cut-off value for CD44v9 IHC staining score were determined using the receiver operating characteristic (ROC) curve. For chi-square test, Pearson's chi-square test or Fisher's exact test were applied. P value of less than 0.05 was considered statistically significant.

Results

Baseline characteristics of study population.

Forty-five paraffin-embedded specimens were obtained from 16 patients with pelvic HGSC (10 ovarian, 4 peritoneal and 2 fallopian tube carcinoma) who underwent surgery in the hospital. Furthermore, normal

FTE tissue from five fibroid patients was included. Detailed information for all patients is provided in **Supplemental Table 1**. The age of the patients with fibroids ranged from 38 to 65 years, with a median of 57 years. The age of the HGSC patients ranged from 41 to 79 years, with a mean of 60 and a median of 59 years. At the time of diagnosis, 81.3% of patients had stage III or worse state of HGSC. Fallopian tube lesions analyzed were located closest to or within 10 mm from the fimbriated end of the fallopian tube. The demographic and clinicopathologic data of the study population are presented in **Table 1**.

Immunohistochemical expression status of p53, CD44v9 and Ki-67.

We investigate the expression of p53 protein, CD44v9 protein and Ki-67 antigen in fallopian tube lesions and HGSC lesions using immunohistochemistry and clarify the correlation of the expression of these markers. Representative images of immunohistochemical staining are shown in **Figure 1**, and the results are numerically shown in **Table 2**. We confirmed that there was no significant difference in the immunohistochemical expression status of p53, CD44v9 and Ki-67 between morphologically normal FTE (n=6) from patients with HGSC and that FTE (n=5) in from patients with benign diseases (data not shown).

First, three cases with p53 complete absence were included in 16 patients with HGSC (**Supplemental Table 1**, case No. 7, 10 and 15). The p53 positivity was identified in HGSC and concomitant p53 signature, dormant STIC and active STIC, but only scattered positive cells were present in normal FTE and SCOUT (**Figure 1, upper panel, Table 2**). p53 signature, dormant STIC, active STIC and HGSC had a significantly higher p53 protein accumulation than normal FTE and SCOUT ($P < 0.001$). There was no significant difference in the p53 protein accumulation among p53 signature, dormant STIC, active STIC and HGSC ($P = 0.342$).

Second, there was a significant lower level of CD44v9 membrane staining and IHC score in dormant STIC, active STIC and HGSC than in normal FTE, SCOUT and p53 signature ($P < 0.001$) (**Figure 1, middle panel, Table 2**). Furthermore, the loss of CD44v9 staining coincided with the appearance of malignant features such as significant nuclear atypia and architectural alterations.

Third, both active STIC and HGSC had a significantly higher Ki-67 index than normal FTE, SCOUT, p53 signature and dormant STIC ($P < 0.001$) (**Figure 1, lower panel, Table 2**). The Ki-67 index in HGSC ranged from 20.0% to 70.0% (median was 40.0%) and the mean \pm SD was $43.4\% \pm 13.5\%$. Active STIC had a Ki-67 index ranging from 30.0% to 50.0%, with a median index of 35.0% and a mean \pm SD of $36.7\% \pm 8.17\%$. There was no significant difference in the Ki-67 labeling index between active STIC and HGSC ($P = 0.255$). Dormant STIC had a low Ki-67 index, ranging from 0% to 5.0%, with a median index of 1.0% and a mean \pm SD of $1.75\% \pm 2.36\%$.

Finally, our data indicate that dual immunostaining for p53 and CD44v9 can reliably identify p53 signature in fallopian tube lesions. Positive p53 / negative CD44v9 immunostaining is a highly specific marker for differentiating dormant STIC, active STIC and HGSC from p53 signature. Twenty-nine (96.7%) of the 30 cases, including 14 STICs and 16 HGSCs, was negative for CD44v9 immunostaining

(**Supplemental Table 1**, Only case 6 is positive for CD44v9). The combined effects of p53 mutations and CD44v9 loss contributes to the progression of p53 signature to dormant STIC. Elevated Ki-67 labeling index is involved in the stepwise evolution from dormant STIC to active STIC, in association with p53 mutations and CD44v9 loss.

Discussion

The current study on HGSC carcinogenesis, based on analyses of precursor lesions, termed SCOUT, p53 signature, dormant STIC, and active STIC lesions, offers two possibilities: first, HGSC develops possibly through a multistep process of genetic or epigenetic alterations, including p53 mutations, followed by CD44v9 loss, then elevated Ki-67 labeling index; and second, each alteration in the evolutionary trajectory of HGSC progression may be acquired independently and sequentially. The current study on HGSC carcinogenesis, based on analyses of precursor lesions, termed SCOUT, p53 signature, dormant STIC, and active STIC lesions, offers the following possibility: HGSC carcinogenesis is a progressive multistep process involving the sequential accumulation of genetic and epigenetic alterations; p53 genetic mutations, followed by CD44v9 loss, then genetic alterations associated with increased Ki-67 labeling index. That is, each alteration in the evolutionary trajectory of HGSC progression may be acquired independently and sequentially. The expression of p53 protein, CD44v9 protein, and Ki-67 antigen was determined by immunohistochemical analysis in morphologically normal FTE and precursor lesions of the fallopian tubes from 16 patients with HGSC. We show that the fallopian tube lesions in HGSC patients displayed distinctive immunophenotypes: 1) normal FTE and SCOUT demonstrated the p53⁻/CD44v9⁺/Ki-67⁻ expression; 2) p53 signature showed the p53⁺/CD44v9⁺/Ki-67⁻ expression; 3) dormant STIC was the p53⁺/CD44v9⁻/Ki-67⁻ expression; and 4) active STIC and HGSC were the p53⁺/CD44v9⁻/Ki-67⁺ expression (**Figure 1**). These immunostaining patterns can reliably identify malignant transformation during the sequential progression from normal FTE and SCOUT to p53 signature, dormant STIC, active STIC, and then HGSC, thereby narrowing the differential diagnosis and elucidating the mechanism of HGSC tumorigenesis. **Figure 2** shows a schematic putative model of HGSC progression based primarily on the current immunohistochemical model. The new finding of this study is that CD44v9 loss may be involved in the progression from p53 signature to dormant STIC.

First, the molecular alterations accumulate in a stepwise manner along the malignant transformation process from normal FTE through precursor lesions to HGSC^{1,23}, but the initial molecular events that lead to transformation from p53 signature to dormant STIC and then active STIC remain poorly understood¹³. The majority of HGSC exhibited high levels of p53 immunoreactivity, and harbored deleterious TP53 mutations²⁴. Nakamura et al. reported that the SCOUT with TP53 mutations progresses to HGSC via the p53 signature and STIC, indicating that TP53 mutations are associated with early events in carcinogenesis of HGSC²⁵. Our study also confirmed that the p53 protein accumulation increased with the progression from SCOUT to p53 signature and then to STIC and invasive cancer.

Second, we explore factors involved in the progression from p53 signature to STIC, because alterations in the p53 protein accumulation or p53 mutations alone do not cause significant nuclear atypia and architectural abnormalities¹³. Our group recently reported that CD44v9 loss may be involved in the progression of endometriosis to type 1 ovarian cancer¹⁷. Malignant transformation of endometriosis occurs mainly through oxidative stress caused by hemorrhage. Similarly, since the fallopian tube epithelial cells are also exposed to the recurrent reflux of menstrual shedding or incessant ovulation, we speculated that redox imbalance is involved in HGSC carcinogenesis. Therefore, we focus on CD44v9 protein as a marker for a sequential progression from normal FTE to precursor lesions and then HGSC. The expression of CD44v9 was lost or significantly reduced in dormant STIC, active STIC and HGSC, suggesting that CD44v9 loss takes part in the progression of p53 signature to dormant STIC (**Figure 1**). As a result of positive clonal selection, the p53⁺/CD44v9⁻ phenotype may be advantageous for survival (**Figure 2**).

We discuss why CD44v9 loss causes nuclear atypia and structural complexity. CD44v9 has been identified as one of the cancer stem cell markers and contributes to ROS defense through up-regulation of the intracellular antioxidant^{8,16,26}. The activation of antioxidant capacities provides protection against oxidative stress and associated diseases, including cancer²⁷. Thus, CD44v9 loss may promote tumorigenesis by enhancing the ROS-induced DNA mutations, which may play an important role in the evolution of STIC^{9,28}. STIC is considered to be susceptible to impaired repair of DNA double-strand breaks, exhibits DNA replication stress and increases genomic instability^{9,28}. The accumulation of genomic instability, including chromosomal instability and copy-number alternations, causes large-scale genomic alterations, leading to HGSC tumorigenesis²⁹.

Why does CD44v9 loss occur in the early stages of STIC lesions? Many regions of the genome exhibit loss of heterozygosity (LOH) in HGSC³⁰. Chromosome arms 11p13, 11p15.5, 11q24, 17p and 17q21 are considered to be regions of frequent LOH³⁰. Since the CD44 gene was mapped to chromosome arm 11p13, CD44v9 loss may be due likely to LOH at 11p13. Another possibility is that CD44v9 downregulation may be attributed to promoter hypermethylation^{31,32}. Verkaik et al. reported that CD44 was hypermethylated and transcriptionally silenced in prostate cancer, suggesting an important role in tumor progression and metastasis³³. However, hypermethylation of CpG islands of CD44v9 has never been reported in HGSC.

To our knowledge, studies from several research groups have pointed out an opposite role of CD44v9. Overexpression of CD44v9 contributes to the aggressive nature of many cancers, including gastric^{34,35}, esophageal³⁶, cholangiocarcinoma³⁷, hepatocellular⁸ and prostate³⁸ cancers, and significantly correlated with the upregulation of p53 and Ki-67 expression³⁴. The expression level of CD44v9 in tumor tissue is significantly associated with the proliferation, invasion, epithelial-mesenchymal transition, aggressiveness and poor prognosis^{8,34-38}. In contrast, our study revealed CD44v9 loss in active STIC and HGSC. The relationship between expression of CD44v9 and tumor aggressiveness is still in a controversial situation. This discrepancy may be due to differences in the function of CD44v9 in cancer and precancerous lesions.

CD44v9 contributes to ROS defenses. In cancer cells, the upregulation of CD44v9 expression is associated with increased aggressive tumor phenotypes. On the other hand, in the early stage of malignant transformation such as active STIC, CD44v9 silencing results in tubal epithelial cell damage due to ovulation and hemorrhage-induced oxidative stress, causing the accumulation of additional genetic alterations, which may be associated with an increased risk of future developing HGSC. However, there are few reports on the importance of CD44v9 expression in precancerous lesions.

Finally, the Ki-67 antigen expression was involved in the stepwise fashion from dormant STIC to active STIC. This finding is consistent with the previous study¹. Ki-67 is one of the molecules that are critical for evaluating the proliferation status and regulating cell cycle progression. Our study identified two immunophenotypes of STIC: the p53⁺/CD44v9⁻/Ki-67⁻ subtype (mostly dormant STIC) and the p53⁺/CD44v9⁻/Ki-67⁺ subtype (mostly active STIC). Active STIC had significantly higher Ki-67 indices than dormant STIC ($P < 0.01$), reflecting the existence of tumor subclones with higher proliferative activity and neoplastic progression. Concurrent alterations of p53 mutations, CD44v9 loss and high mitotic index may be associated with a more proliferative immunophenotype in STIC. However, it is unknown at this time which genetic alterations cause the malignant behavior of the dormant STIC to the active STIC, but there are several possibilities. Few studies have analyzed the genetic and molecular alterations from dormant STIC to active STIC¹³. Subsequent to CD44v9 loss, deletion of the tumor suppressor genes located within and in close proximity to known deleted area at chromosome arm 11p13 may cause malignant behavior of dormant STIC to active STIC. A potential candidate gene at this locus is Wilms' tumor 1 (WT1), a proposed tumor-suppressor gene, but this gene did not reveal any abnormalities in ovarian cancer³⁹. Allelic imbalance for other tumor suppressor genes involving chromosome 11p13 may be an early event in active STIC lesion formation. Alternatively, CD44v9 loss itself may cause an accumulation of mutations in other genes and subsequent carcinogenesis, which may influence pre-neoplastic changes in gene expression relevant to nuclear atypia, architectural alterations and tumor development.

In conclusion, STIC lesions may progress through the acquisition of sequential changes in p53 mutations, CD44v9 loss, and elevated Ki-67 expression. We propose the following hypothesis for multi-stage carcinogenesis of HGSC: the progression from p53 signature to dormant STIC is caused by CD44v9 loss following p53 gene mutation. Subsequently, progression from dormant STIC to active STIC may require additional genetic mutations that can trigger Ki-67 overexpression. Future studies are needed to assess the underlying mechanism of CD44v9 loss and to identify the genetic mutations involved in the transition from dormant STIC to active STIC during the process of carcinogenesis.

Acknowledgements

The authors are grateful to Masako Nakata from Laboratory of Diagnostic Pathology at Nara Medical University for technical assistance with immunohistostaining.

Author's contribution

SS and TU evaluated the results of the immunohistochemical staining.

CO was in charge of experimental guidance.

SS, TU, NK and HK performed the literature search.

NK was responsible for statistical processing of the data.

SS and HK made substantial contribution to conception of the study and wrote a draft of this manuscript.

The final version of the manuscript has been read and approved by all authors.

References

1. Mittal N, Srinivasan R, Gupta N, et al. Secretory cell outgrowths, p53 signatures, and serous tubal intraepithelial carcinoma in the fallopian tubes of patients with sporadic pelvic serous carcinoma. *Indian J Pathol Microbiol.* 2016;59(4):481-488.
2. Saini U, Suarez AA, Naidu S, et al. STAT3/PIAS3 Levels Serve as "Early Signature" Genes in the Development of High-Grade Serous Carcinoma from the Fallopian Tube. *Cancer Res.* 2018;78(7):1739-1750.
3. Eckert MA, Pan S, Hernandez KM, et al. Genomics of Ovarian Cancer Progression Reveals Diverse Metastatic Trajectories Including Intraepithelial Metastasis to the Fallopian Tube. *Cancer Discov.* 2016;6(12):1342-1351.
4. McDaniel AS, Stall JN, Hovelson DH, et al. Next-Generation Sequencing of Tubal Intraepithelial Carcinomas. *JAMA Oncol.* 2015;1(8):1128-1132.
5. Kuhn E, Kurman RJ, Vang R, et al. TP53 mutations in serous tubal intraepithelial carcinoma and concurrent pelvic high-grade serous carcinoma--evidence supporting the clonal relationship of the two lesions. *J Pathol.* 2012;226(3):421-426.
6. Vang R, Visvanathan K, Gross A, et al. Validation of an algorithm for the diagnosis of serous tubal intraepithelial carcinoma. *Int J Gynecol Pathol.* 2012;31(3):243-253.
7. Visvanathan K, Vang R, Shaw P, et al. Diagnosis of serous tubal intraepithelial carcinoma based on morphologic and immunohistochemical features: a reproducibility study. *Am J Surg Pathol.* 2011;35(12):1766-1775.
8. Wada F, Koga H, Akiba J, et al. High expression of CD44v9 and xCT in chemoresistant hepatocellular carcinoma: Potential targets by sulfasalazine. *Cancer Sci.* 2018;109(9):2801-2810.
9. Kobayashi H, Ogawa K, Kawahara N, et al. Sequential molecular changes and dynamic oxidative stress in high-grade serous ovarian carcinogenesis. *Free Radic Res.* 2017;51(9-10):755-764.
10. Chen EY, Mehra K, Mehrad M, et al. Secretory cell outgrowth, PAX2 and serous carcinogenesis in the Fallopian tube. *J Pathol.* 2010;222(1):110-116.
11. Kindelberger DW, Lee Y, Miron A, et al. Intraepithelial carcinoma of the fimbria and pelvic serous carcinoma: Evidence for a causal relationship. *Am J Surg Pathol.* 2007;31(2):161-169.
12. Crum CP. Intercepting pelvic cancer in the distal fallopian tube: theories and realities. *Mol Oncol.* 2009;3(2):165-170.
13. Wu RC, Wang P, Lin SF, et al. Genomic landscape and evolutionary trajectories of ovarian cancer precursor lesions. *J Pathol.* 2019;248(1):41-50.
14. Fathalla MF. Incessant ovulation and ovarian cancer - a hypothesis re-visited. *Facts Views Vis Obgyn.* 2013;5(4):292-297.
15. Iwabuchi T, Yoshimoto C, Shigetomi H, Kobayashi H. Oxidative Stress and Antioxidant Defense in Endometriosis and Its Malignant Transformation. *Oxid Med Cell Longev.* 2015;2015:848595.

16. Mvunta DH, Miyamoto T, Asaka R, et al. SIRT1 Regulates the Chemoresistance and Invasiveness of Ovarian Carcinoma Cells. *Transl Oncol*. 2017;10(4):621-631.
17. Niiro E, Kawahara N, Yamada Y, et al. Immunohistochemical expression of CD44v9 and 8-OHdG in ovarian endometrioma and the benign endometriotic lesions adjacent to clear cell carcinoma. *J Obstet Gynaecol Res*. 2019;45(11):2260-2266.
18. Kurman RJ, Shih Ie M. The origin and pathogenesis of epithelial ovarian cancer: a proposed unifying theory. *Am J Surg Pathol*. 2010;34(3):433-443.
19. Kobel M, Reuss A, du Bois A, et al. The biological and clinical value of p53 expression in pelvic high-grade serous carcinomas. *J Pathol*. 2010;222(2):191-198.
20. Kobel M, Piskorz AM, Lee S, et al. Optimized p53 immunohistochemistry is an accurate predictor of TP53 mutation in ovarian carcinoma. *J Pathol Clin Res*. 2016;2(4):247-258.
21. Hsu CP, Lee LY, Hsu JT, et al. CD44 Predicts Early Recurrence in Pancreatic Cancer Patients Undergoing Radical Surgery. *In Vivo*. 2018;32(6):1533-1540.
22. Kuhn E, Kurman RJ, Sehdev AS, Shih Ie M. Ki-67 labeling index as an adjunct in the diagnosis of serous tubal intraepithelial carcinoma. *Int J Gynecol Pathol*. 2012;31(5):416-422.
23. Nakamura K, Nakayama K, Ishikawa N, et al. Reconstitution of high-grade serous ovarian carcinoma from primary fallopian tube secretory epithelial cells. *Oncotarget*. 2018;9(16):12609-12619.
24. Chien J, Sicotte H, Fan JB, et al. TP53 mutations, tetraploidy and homologous recombination repair defects in early stage high-grade serous ovarian cancer. *Nucleic Acids Res*. 2015;43(14):6945-6958.
25. Nakamura M, Obata T, Daikoku T, Fujiwara H. The Association and Significance of p53 in Gynecologic Cancers: The Potential of Targeted Therapy. *Int J Mol Sci*. 2019;20(21).
26. Nagano O, Okazaki S, Saya H. Redox regulation in stem-like cancer cells by CD44 variant isoforms. *Oncogene*. 2013;32(44):5191-5198.
27. Yang Y, Yee D. IGF-I regulates redox status in breast cancer cells by activating the amino acid transport molecule xC. *Cancer Res*. 2014;74(8):2295-2305.
28. Liu Z, Liu J, Segura MF, et al. MiR-182 overexpression in tumorigenesis of high-grade serous ovarian carcinoma. *J Pathol*. 2012;228(2):204-215.
29. Zhang H, Liu T, Zhang Z, et al. Integrated Proteogenomic Characterization of Human High-Grade Serous Ovarian Cancer. *Cell*. 2016;166(3):755-765.
30. Pedersen BS, Konstantinopoulos PA, Spillman MA, De S. Copy neutral loss of heterozygosity is more frequent in older ovarian cancer patients. *Genes Chromosomes Cancer*. 2013;52(9):794-801.
31. Kito H, Suzuki H, Ichikawa T, et al. Hypermethylation of the CD44 gene is associated with progression and metastasis of human prostate cancer. *Prostate*. 2001;49(2):110-115.
32. Sato S, Yokozaki H, Yasui W, Nikai H, Tahara E. Silencing of the CD44 gene by CpG methylation

- in a human gastric carcinoma cell line. *Jpn J Cancer Res.* 1999;90(5):485-489.
33. Verkaik NS, Trapman J, Romijn JC, Van der Kwast TH, Van Steenbrugge GJ. Down-regulation of CD44 expression in human prostatic carcinoma cell lines is correlated with DNA hypermethylation. *Int J Cancer.* 1999;80(3):439-443.
 34. Yasui W, Kudo Y, Naka K, et al. Expression of CD44 containing variant exon 9 (CD44v9) in gastric adenomas and adenocarcinomas: relation to the proliferation and progression. *Int J Oncol.* 1998;12(6):1253-1258.
 35. Jang BI, Li Y, Graham DY, Cen P. The Role of CD44 in the Pathogenesis, Diagnosis, and Therapy of Gastric Cancer. *Gut Liver.* 2011;5(4):397-405.
 36. Taniguchi D, Saeki H, Nakashima Y, et al. CD44v9 is associated with epithelial-mesenchymal transition and poor outcomes in esophageal squamous cell carcinoma. *Cancer Med.* 2018;7(12):6258-6268.
 37. Suwannakul N, Ma N, Thanan R, et al. Overexpression of CD44 Variant 9: A Novel Cancer Stem Cell Marker in Human Cholangiocarcinoma in Relation to Inflammation. *Mediators Inflamm.* 2018;2018:4867234.
 38. Ghatak S, Hascall VC, Markwald RR, Misra S. Stromal hyaluronan interaction with epithelial CD44 variants promotes prostate cancer invasiveness by augmenting expression and function of hepatocyte growth factor and androgen receptor. *J Biol Chem.* 2010;285(26):19821-19832.
 39. Viel A, Giannini F, Capozzi E, et al. Molecular mechanisms possibly affecting WT1 function in human ovarian tumors. *Int J Cancer.* 1994;57(4):515-521.

Supplemental Table 1. Detailed baseline characteristics and immunohistochemical staining results for each patient.

Table 1. Baseline characteristics of study subjects

Table 2. Immunohistochemical expression status in p53 protein, CD44v9 IHC score and Ki-67 labeling index in fallopian tube lesions and HGSC.

The significance of the difference of the immunohistochemical expression status obtained in paired samples was estimated according to the Kruskal-Wallis test followed by the Steel-Dwass test. CD44v9 IHC score: Normal vs. dormant STIC, $p=0.022$; Normal vs. active STIC, $p=0.039$; Normal vs. HGSC, $p=0.010$; SCOUT vs. dormant STIC, $p=0.034$; SCOUT vs. HGSC, $p=0.011$; and P53 signature vs. HGSC, $p=0.028$. p53 protein: Normal vs. dormant STIC, $p=0.018$; Normal vs. active STIC, $p=0.025$; SCOUT vs. dormant STIC, $p=0.029$; and SCOUT vs. active STIC, $p=0.032$. Ki-67 labeling index: Normal vs. active STIC, $p=0.040$; Normal vs. HGSC, $p=0.005$; SCOUT vs. HGSC, $p=0.010$; P53 signature vs. HGSC, $p=0.026$; Dormant STIC vs. active STIC, $p=0.019$; and Dormant STIC vs. HGSC, $p=0.001$.

Figure Legend.

Figure 1. Immunohistochemical expression status of p53, CD44v9 and Ki-67 in samples of normal FTE, SCOUT, p53 signature, dormant STIC, active STIC, and HGSC.

This figure shows representative immunostaining results of p53, CD44v9 and Ki-67. The results of immunostaining of normal FTE and SCOUT are negative for p53 expression ($p53^-$), positive for CD44v9 expression ($CD44v9^+$), and negative for the Ki-67 antigen ($Ki-67^-$). The p53 signature lesions are $p53^+$, $CD44v9^+$, and $Ki-67^-$ (black arrowhead). The dormant STIC lesions are $p53^+$, $CD44v9^-$, and $Ki-67^-$ (black arrowhead). Normal FTE adjacent to dormant STIC is $p53^-$, $CD44v9^+$ and $Ki-67^-$ (white arrowhead). The active STIC lesions are $p53^+$, $CD44v9^-$, and $Ki-67^+$ (black arrowhead). Normal FTE adjacent to active STIC is $p53^-$, $CD44v9^+$ and $Ki-67^-$ (white arrowhead).

Figure 2. A schematic putative model of HGSC progression based on sequential molecular alterations.

This figure illustrates the schematic immunophenotype model in an evolutionary pathway of HGSC tumorigenesis. Normal fallopian tube epithelial cells express the CD44v9 protein to ameliorate oxidative stress. Accumulation of p53 mutations is required for the development of p53 signature lesions. In addition, CD44v9 loss may trigger the progression from p53 signature to dormant STIC lesions. The dormant STIC, which has a clonal increase in proliferative capacity, can then promote carcinogenesis through active STIC lesions. HGSC develops through a particular sequence of genetic alterations (p53 mutations, followed by CD44v9 loss, and then Ki-67 overexpression). The evolutionary trajectory of HGSC progression indicates

a multistage carcinogenesis, as each alteration is acquired independently. red, nuclear p53 protein accumulation >75%; blue, CD44v9 IHC score >150; and green, Ki-67 labeling index \geq 10%.

Table 1.

Parameters	HGSC patients	Controls
Age at diagnosis, median (range), year	59.0 (41–79)	57.0 (38–65)
Parity		
0	3	1
1	2	1
>1	11	3
BMI, median (range), kg/m ²	22.0 (17.1–27.7)	26.3 (20.6–31.2)
Menopausal status		
Yes	12	3
No	4	2
FIGO stage, patients number (%)		
I	2 (12.5)	
II	1 (6.25)	
III	10 (62.5)	
IV	3 (18.75)	
Diagnosis		
Ovarian	10	Fibroids (n=5)
Peritoneal	4	
Fallopian	2	

Table 2.

Protein expression		normal FTE	SCOUT	p53 signature	dormant STIC	active STIC	HGSC	p value
Total samples, n		11	5	4	8	6	16	
p53 positivity	n (%), median, range	0 (0%), 20.0, 5-40	0 (0%), 20.0, 10-25	4(100%), 92.5, 90-95	8(100%), 95.0, 80-95	6(100%), 95.0, 95-95	16 (100%), 95.0, 0-95	P<0.001***
CD44v9, IHC score	median, range	270, 210-300	200, 200-300	250, 180-300	25.0, 0-140	3.00, 0-90	30, 0-120	P<0.0001***
Ki-67 positivity	n (%), median, range	0 (0%), 2.0, 1-5	0 (0%), 0.0, 0-2	0 (0%), 1.0, 0-5	0 (0%), 3.5, 0-5	6 (100%), 35.0, 30-50	16 (100%), 40.0, 20-70	P<0.0001***

Figure 1.

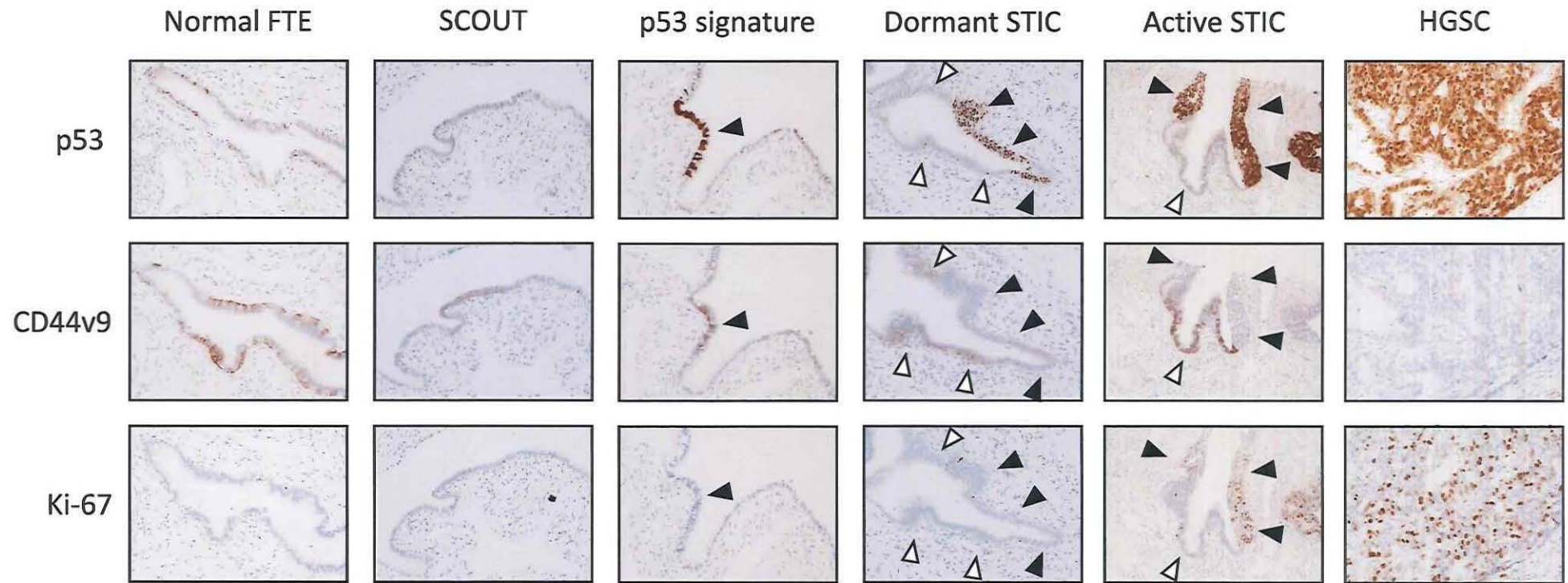


Figure 2.

